dt/dΔ Measurement of Short Period P Waves in the Upper Mantle for the Western North America using LASA

by

Jack Christian Wolfe

B.S., University of Southern California
(1967)

B.A., University of Southern California
(1967)

SUBMITTED IN PARTIAL FULFILLMENT

OF THE REQUIREMENTS FOR THE

DEGREE OF MASTER OF SCIENCE

at the

MASSACHUSETTS INSTITUTE OF TECHNOLOGY

(November, 1969)
i.e. Dec. 1969

Signature of Author. . . . . .
Department of Earth and Planetary Sciences, Nov. 14, 1969

Certified by . . . . . .
Thesis Supervisor

Accepted by . . . . . .
Chairman, Departmental Committee on Graduate Students

Report Documentation Page

Form Approved
OMB No. 0704-0188

1. REPORT DATE	2. REPORT TYPE	3. DATES COVERED
NOV 1969		**00-00-1969 to 00-00-1969**

4. TITLE AND SUBTITLE	5a. CONTRACT NUMBER
dt/d Measurement of Short Period P Waves in the Upper Mantle for the Western North America using LASA	5b. GRANT NUMBER
	5c. PROGRAM ELEMENT NUMBER
6. AUTHOR(S)	5d. PROJECT NUMBER
	5e. TASK NUMBER
	5f. WORK UNIT NUMBER
7. PERFORMING ORGANIZATION NAME(S) AND ADDRESS(ES) **Massachusetts Institute of Technology,77 Massachusetts Avenue,Cambridge,MA,02139**	8. PERFORMING ORGANIZATION REPORT NUMBER
9. SPONSORING/MONITORING AGENCY NAME(S) AND ADDRESS(ES)	10. SPONSOR/MONITOR'S ACRONYM(S)
	11. SPONSOR/MONITOR'S REPORT NUMBER(S)

12. DISTRIBUTION/AVAILABILITY STATEMENT
Approved for public release; distribution unlimited

13. SUPPLEMENTARY NOTES

14. ABSTRACT

15. SUBJECT TERMS

16. SECURITY CLASSIFICATION OF:			17. LIMITATION OF ABSTRACT	18. NUMBER OF PAGES	19a. NAME OF RESPONSIBLE PERSON
a. REPORT	b. ABSTRACT	c. THIS PAGE			
unclassified	**unclassified**	**unclassified**	**Same as Report (SAR)**	**60**	

ABSTRACT

Seismic ray parameter ($dt/d\Delta$) has been measured in the distance range Δ = 8-34° utilizing LASA. An upper mantle velocity structure for P waves applicable to the Western Part of North America has been derived from these data. Measurement of $dt/d\Delta$ was accomplished by calculating with a least squares procedure the $dt/d\Delta$ from the measured arrival time at each sub-array or by forming beams with LASA from which $dt/d\Delta$ was picked from the beams that gave the maximum amplitude. The velocity models were calculated by a Monte Carlo technique and show a low velocity region centered at a depth of 120 km and two zones of rapid velocity increase at 350 km and 650 km where the velocity changes from 8.7 to 9.6 km/sec and 10.2 to 10.9 km/sec, respectively. Our $dt/d\Delta$ data supports the accumulating evidence that $dt/d\Delta$ is azimuthally dependent at LASA. Also, the data suggests that this azimuthal dependence is a result of structural anisotropy under LASA.

Thesis Supervisor: M. Nafi Toksöz
Title: Associate Professor of Geophysics

ACKNOWLEDGEMENTS

The author expresses his appreciation to Professor Nafi Toksöz who provided advice and assistance during this study and who was the author's thesis advisor. Dr. Ralph Wiggins' computer programs were used to invert the data in this study. The author also thanks Professor Shawn Biehler and Drs. Robert Sheppard, Don Helmberger, and John Fairborn for providing computer programs and valuable discussions pertinent to the conclusion of this study. Finally, I would like to thank Misses Tasha and Thalia Lingos who typed and grammatically corrected the many revisions of the manuscript.

The staff of Group 64 at Massachusetts Institute of Technology Lincoln Laboratory provided the data used in this study and the computational facilities. The research was supported by the Advanced Research Projects Agency and monitored by the Air Force Office of Scientific Research under contract AF 49(638)-1632.

Table of Contents

List of Tables and Figures

I. INTRODUCTION

Much attention has been given to the detailed compressional or body wave velocity structure of the upper mantle, especially with regard to the "low velocity" zone and the two sharp velocity increases at depths of 350 km and 650 km. This velocity distribution in the upper mantle has been obtained from studying travel-time curves and dispersion of seismic surface waves. Most of the recent velocity distribution studies have been directed towards a detailed description of a travel-time curve, using nuclear events and explosions (Lewis and Meyer, 1968; Green and Hales, 1968). However, the difficulty in determining the absolute arrival time of latter phases from the triplication of the travel-time curve has limited the interpretation of details of the velocity structure. Reviews by Nuttli (1963), Saverenski (1960), Anderson (1965, 1967), and Julian and Anderson (1967) summarize these efforts.

With the advent of seismic arrays, the travel-time derivative ($p = dt/d\Delta$) of seismic body waves can be measured, without any need for determining the absolute arrival-time of a wave. This ray parameter, $dt/d\Delta$, also known as wave slowness, is inversely proportional to the phase velocity. Advantages of using $dt/d\Delta$ measurements are that source and depth corrections have little effect on the results (Chinnery and Toksöz, 1967); and the absolute arrival time need not be known, since only a

recognizable waveform which can be identified across the array is needed. Also, the phase velocity gives us a direct measurement of velocity at the bottom of the ray path (Bullen, 1963). This parameter, p, is insensitive to layering around the source, but it is affected by lateral variations along the bottom of the ray path. For this investigation, we have measured the travel-time derivative ($dt/d\Delta$) in the western North America of first and later arrivals using Large Aperture Seismic Array (LASA) in the distance range of $\Delta = 8°$ to $34°$. Also, we observed the approximate arrival times and amplitude of these refracted waves.

Some recent studies which have used arrays to measure $dt/d\Delta$ up to distances of $\Delta = 40°$ are those of Kanamori (1967), Johnson (1967), and Niazi and Anderson (1965). The last two are investigations done in the same approximate area as this study, western North America. The main difference in this study, as contrasted to previous studies, is the size (200 km) and the symmetry of LASA, and the use of more advanced digital processing techniques.

Typically, the $dt/d\Delta$ data is inverted by a method described by Bullen (1960, 1963) and is known as the Weichert-Herglotz formula. However, this method fails if there is a low velocity zone in a velocity structure and, as the data suggests, this zone occurs below the Moho boundary in tectonic areas (Lehmann, 1962). If a low

velocity zone is postulated, the non-uniqueness of solution can be visualized by observing that if one increases the average velocity of the zone in order to satisfy the travel-time curves, one must make the zone thicker. Dowling and Nuttli (1964) quantitatively explored travel-time curves resulting from varied thicknesses of low velocity zones, and found that limits can be placed on the extent of the low velocity zone from the travel-time curves.

A way in which to detect the thickness of this zone was suggested by Gutenberg (1953). His method entails the observation of a series of events that have sources at different depths extending through the low velocity zone. Gutenberg's method cannot be applied to the present study because of the shallow nature of the events from the source regions. One method to circumvent this fact was used by Johnson (1967), where he "stripped" the earth down to below this zone, then inverted his data. In contrast to Johnson's inversion technique, inversion of the data collected in this paper was accomplished by a procedure described by Wiggins (1969). His scheme is a Monte Carlo technique that generates random velocity models for the upper mantle, which are inverted and tested to see if they satisfy the travel-time, and the $dt/d\Delta$ values observed. The chief value of this method is that it will generate a set of velocity models that will satisfy the measured

constraints. We can then look at the similarity between the models and compare them to existing models.

Before we compare our models to those of Johnson (1967) and Kanamori (1967), we must note that Toksöz, et al. (1967) have shown that lateral inhomogeneities exist in the upper mantle. Western North America is quite likely to be subject to these lateral variations in apparent phase velocity. One would expect, since we used $dt/d\Delta$ data from over all the western azimuths (160° to 350°) from LASA, that we are presenting an average compressional wave velocity model for this region.

The remainder of this thesis is divided into three parts dealing with our data, our method of analysis, and our conclusions. Our data section, Chapter II, deals with the acquisition of our data and the standard corrections that we have applied to the data. In Chapter III, the analysis section, we discuss the "stacking" and "plotting" methods we used to gather our data. In this section we make observations about LASA and how the current model for its anisotropic structure does not bring our data into accord. Also, the corrected values of $dt/d\Delta$ are presented along with our derived velocity models. A summary of the results and conclusions from our data and analysis are given in Chapter IV.

II. DATA

The data for this study were collected on digital magnetic tape from LASA, which consists of twenty-one sub-arrays and is located in western United States. The digitizing interval is .05 seconds and, combined with LASA's approximately 200-km aperture, gives a theoretical error of .04 sec/deg in ray parameter measurements. Details of the instrumentation can be found in Green, et al. (1965); Briscoe and Fleck (1965); and Capon, et al. (1968).

A continuous record of all sub-arrays at LASA is retained on "develocorder" films. Because of the inacuracies and optical distortions inherent in the analog transcriptions of data, these films were only used when critical events occurred for which, for one reason or another, no magnetic tape existed.

Our data was gathered from the Lincoln Laboratory Group 64 library of seismic events. Approximately six hundred events from 8° to 34° were analyzed for the interval from June, 1965 to December, 1968, of which ninety were suitable for $dt/d\Delta$ measurement. The list of these measurable events is given in Table 1. Additional data, such as origin time and hypocenter were obtained from the Preliminary Determination of Epicenter (PDE) cards published by the United States Coast and Geodetic Survey (USCGS). From the latitude and longitude given from the

Table 1. List of events.

EVENT NO.	DATE	ORIGIN TIME	MAG.	DEPTH KM	DISTANCE DEG	AZIMUTH DEG
1	2- 9-66	21:20:16.6	5.2	34	20.18	191
2	9-12-65	6: 7:47.6	6.0	54	29.76	168
3	26-11-66	4:30:57.8	4.6	33	15.36	252
4	26-11-66	5:56:39.1	4.6	33	15.23	252
5	1-12-66	4:29:23.2	4.6	38	26.97	314
6	13- 4-67	19:59:51.9	5.6	86	28.55	167
7	14- 4-67	5:18:35.7	4.9	62	29.53	168
8	29- 4-67	0: 4:41.7	5.1	6	16.48	294
9	5- 5-67	17: 6:14.8	4.9	102	28.80	321
10	3- 6-67	9: 8:56.3	5.5	32	29.19	310
11	24- 6-67	14:28:52.6	4.5	97	28.71	167
12	7- 8-67	11:14:42.7	5.1	33	30.98	310
13	9- 8-67	13:25: 6.2	5.3	5	6.88	170
14	27- 8-67	18:29: 7.4	4.1	33	15.95	290
15	7- 9-67	12:39:17.2	4.9	10	15.02	235
16	13- 9-67	20:46:11.7	4.7	33	26.93	186
17	17- 9-67	7:56:22.7	5.2	45	31.07	157
18	17- 9-67	16:49: 2.3	4.4	33	16.71	205
19	21- 9-67	0: 1:54.1	5.1	33	17.18	209
20	28- 9-67	15:44:55.6	5.6	28	27.21	313
21	4-10-67	10:20:14.0	5.2	18	9.26	210
22	17-10-67	14:53:25.2	4.2	33	21.81	314
23	4-11-67	16: 2:19.3	4.7	33	26.13	313
24	27-11-67	4:27: 2.4	4.6	16	24.32	316
25	27-11-67	5: 9:22.7	5.2	5	6.78	170
26	2-12-67	0:31:18.8	5.1	33	22.67	185
27	4-12-67	8:48:45.1	4.6	33	15.22	266
28	5-12-67	11: 9:37.3	5.0	33	17.00	203
29	5-12-67	18:35:37.5	4.8	33	16.97	203
30	10-12-67	12:33:54.1	4.6	15	14.93	252
31	18-12-67	17:24:31.8	5.0	11	15.09	235
32	10-12-67	19:30: 0.1	5.1	0	10.01	185
33	28-12-67	6:26:15.7	5.4	33	16.03	269
34	28-12-67	7: 1:36.7	4.9	33	16.17	269
35	28-12-67	22:11:33.8	5.0	33	16.10	269
36	30-12-67	8: 4:43.2	4.6	33	14.48	251
37	3- 1-68	10:18: 0.6	4.7	19	27.09	313
38	19- 1-68	18:14:56.0	6.3	0	10.51	227
39	19- 1-68	20:23:37.8	4.6	33	14.77	264
40	26- 1-68	12:30:46.2	5.3	33	22.74	192
41	30- 1-68	15:20: 5.5	4.5	18	9.87	238
42	1- 2-68	7:58: 3.5	5.4	14	16.01	291
43	2- 2-68	20:15:25.6	5.0	25	28.84	278
44	3- 2-68	5:36:14.5	5.7	9	30.44	167
45	20- 2-68	2:45:49.2	3.9	33	24.80	315
46	2- 3-68	3:14:44.5	5.1	33	15.53	287
47	25- 3-68	11:32: 7.0	4.5	8	14.27	232
48	9- 4-68	2:28:58.9	6.1	20	15.53	212

Table 1, continued

EVENT NO.	DATE	ORIGIN TIME	MAG.	DEPTH KM	DISTANCE DEG	AZIMUTH DEG
49	9- 4-68	3: 3:55.4	5.1	15	15.40	212
50	23- 4-68	20:29:14.5	6.3	23	28.58	310
51	26- 4-68	15: 2:30.0	0.0	0	0.00	219
52	8- 5-68	12:16:59.0	4.9	0	17.43	264
53	5- 7-68	19:33:10.3	4.1	28	27.43	316
54	6- 7-68	14: 2:42.0	5.1	33	9.88	239
55	23- 7-68	18:28: 1.2	5.4	33	27.92	181
56	2- 8-68	14: 6:43.9	6.3	40	30.83	164
57	2- 8-68	18:37:52.0	5.0	33	31.31	164
58	29- 8-68	22:48: 0.0	0.0	0	0.00	218
59	15- 9-68	11:27:36.5	3.9	0	13.69	265
60	9-11-68	17: 1:41.1	5.3	19	15.74	117
61	25-11-68	0:53: 1.3	5.0	0	26.44	186
62	19-12-68	16:33:30.0	0.0	0	0.00	219
63	8- 4-66	9:19: 9.6	4.7	33	29.60	307
64	10- 4-66	22:27: 1.7	5.6	33	14.80	256
65	11- 4-66	17:17:33.7	5.7	72	28.40	172
66	16- 4-66	1:27:15.3	5.7	33	30.40	307
67	30- 4-66	13: 1:18.5	5.2	54	27.80	181
68	6- 5-66	15: 0: 0.0	5.0	0	12.00	222
69	18- 5-66	7:32: 7.2	5.3	33	21.80	187
70	20- 5-66	23:58:51.7	5.0	37	16.00	291
71	22- 5-66	7:42:49.9	5.5	53	25.50	185
72	22- 5-66	9:29:22.7	5.2	48	25.60	185
73	23- 5-66	11:51:29.6	5.6	58	25.30	185
74	3- 6-66	14: 0: 0.0	5.0	0	12.00	220
75	22- 6-66	7:11: 0.7	5.1	87	34.00	155
76	22- 6-66	11:38:53.7	5.2	53	27.80	317
77	30- 6-66	22:15: 0.1	6.0	0	12.00	222
78	7- 7-66	22:30: 5.1	5.0	18	15.40	267
79	14- 7-66	12:18:17.0	5.2	33	28.30	305
80	7- 8-66	17:36:26.7	5.8	33	16.20	206
81	16- 8-66	18: 2:36.1	6.0	33	11.00	215
82	17-12-66	18: 0:22.0	4.6	0	13.10	77
83	15- 2-67	3:28: 3.5	4.4	5	6.90	198
84	23- 2-67	18:49:29.0	4.8	0	14.70	213
85	14- 4-67	10: 4:17.2	4.2	33	21.20	188
86	19- 4-67	18:12:24.6	4.3	33	17.30	299
87	29- 4-67	0: 4:41.8	6.0	6	16.50	294
88	29- 4-67	0: 7:53.2	4.9	33	15.30	267
89	20- 5-67	14:59:49.0	5.6	0	13.00	218
90	15- 7-67	11:56: 9.0	4.5	0	21.90	189
91	9- 8-67	13:25: 6.2	5.8	5	6.90	170
92	13- 8-67	16:44:22.3	5.0	33	15.00	265

PDE cards, the distance and azimuth were calculated for each event.

Seismicity and the differences in mantle structure between eastern and western North America constrained our measurements to the west of LASA as shown in Figure 1. Therefore, ray paths for the events used in this study bottom in western North America (Western Cordillera), sometimes called a "mountain tectonic" region (Toksöz, et al., 1967). Distinguishing geophysical features of this area are: (1) a generally low P_n, 7.8 km/sec (Carder, et al., 1966), which varies from 7.8 to 8.1 km/sec (as contrasted to an eastern continental velocity of greater than 8.1 km/sec); (2) a higher heat flow (2 HFU) than in the East (1.2 HFU), (Birch, et al., 1968; Roy, et al., 1968); (3) a low electrical conductivity layer which decreases from 150 km deep to 50 km, from east to west, near the Rocky Mountain and Great Plains boundary, as suggested by the magnetotelluric data collected by Schmucker (1964) and Reitzel (1967); (4) a lack of the low frequency magnetic anomalies, observed by Zeitz, et al. (1966), (a possible correlation to heat flow due to the Curie isotherm coming closer to the earth's surface); (5) finally, on a regional scale, an achievement of isostatic adjustment as deduced from the free-air and Bouguer gravity anomalies (Woollard, 1959).

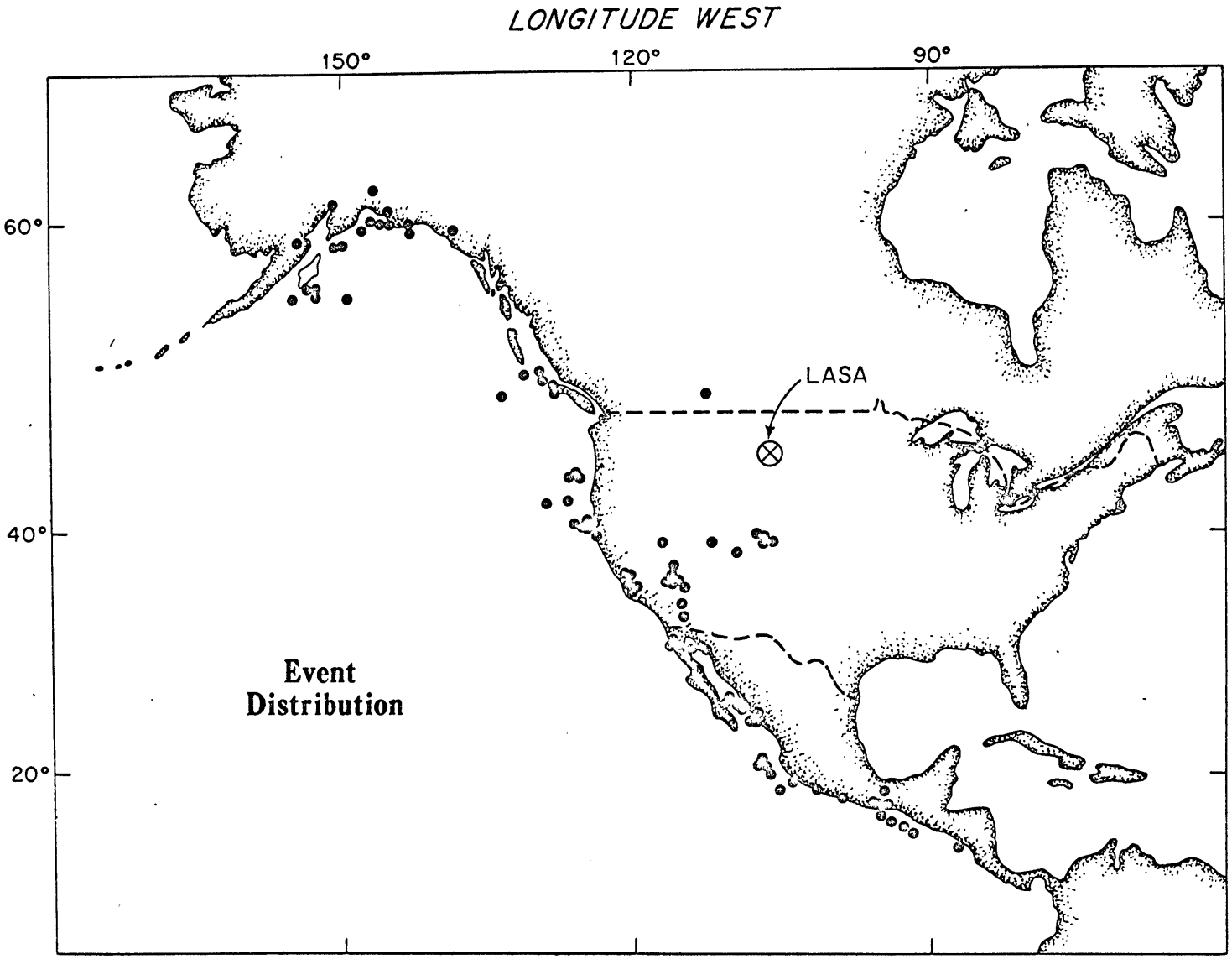

Figure 1. Distribution of events.

Two corrections were applied to the data. The first correction was an azimuthal correction for our $dt/d\Delta$ measurements and is discussed in the Analysis section, Chapter III. The second correction was utilized to reduce each event to a standard depth. Since most of our events occurred in the 30 km depth range, we adjusted the hypocenter for each event to 30 km in order to minimize the error in the hypocenter correction.

To calculate the depth correction, we used the measured value of $dt/d\Delta$, the depth from the PDE cards, and a velocity model averaged from Pakiser and Steinhart's (1964) data. We ray-traced from the hypocenter to a 30 km depth and computed the change in surface distance, which was then added (algebraically) to the distance calculated from the PDE cards. The crustal model used is:

Depth (km)	Velocity (km/sec)
0 - 15	6.0
15 - 40	6.4
40 - 100	7.9
100 ---	8.0

Extremes in possible crustal velocities from this model changed the corrected value by less than 0.1 degrees, which was deemed satisfactory, considering the accuracy of depth determination of shallow focus earthquakes.

A summary of the geology of the area around LASA was

done by Brown and Poort (1965). They observed that the central LASA region is situated on 3200 meters of undisturbed sediments, lying conformably on Precambrian basement. They also noted that some structural deformation exists at the eastern and western extremities of the region. Their data shows that P-wave velocities average less than 3 km/sec in the Mesozoic sediments to depths on the order of 1900 meters, and average 5.8 km/sec in the Paleozoic rocks below that depth. Zeitz, et al. (1968), in their preliminary interpretation of the magnetic and gravity data for LASA, found that magnetic and gravity anomalies are associated with a dome structure beneath the E_4 sub-array, and that the LASA area may be defined by five major crustal units, separated by fault-like boundaries that extend into the Precambrian basement. Their preliminary gravity data shows LASA to have a -100 mgals Bouguer regional anomaly and to be an area of high frequency and low amplitude (10 mgals) anomalies. Unfortunately this gravity investigation was not extended beyond the boundaries of LASA. Consequently, we made no attempt to remove regional gradients in order to look at some of the lower frequency gravity anomalies coming from the crust-mantle boundary. Finally, from seismic refraction work done across LASA, Borcherdt and Roller (1967), and Steinhart and Meyers (1961) developed two different

velocity structures. These surveys are approximately perpendicular to each other.

The next chapter investigates this azimuthal anisotropy, our azimuthal correction, and our methods of measuring $dt/d\Delta$ for later arrivals.

III. ANALYSIS

To measure $dt/d\Delta$ from the events in Table 1, two methods were employed. Our first method used digital magnetic tape from LASA, Calcomp plots of each event, and a special purpose PDP-7 computer. This technique was used when an arrival was observable across the entire array. Our other method for recovering $dt/d\Delta$ used a "beam forming" process that discriminated between arrivals that were difficult to trace across the array. This procedure will also be discussed.

To facilitate the discussion of $dt/d\Delta$, we have used the inverse apparent phase velocity in sec/deg. In Table 2 we have listed the conversion of sec/deg to km/sec. For this conversion we used:

$$p(\text{sec/deg}) * VP(\text{km/sec}) = 111.19. \qquad \text{(III.1)}$$

To calculate the $dt/d\Delta$ from travel-times measured at each sub-array, we used a least squares procedure. To perform our least squares solution for a plane wave, we set the center of LASA the A_0 sub-array, as the coordinate origin. Hence, we have the spatial coordinates X_i' and Y_i', and the time, T_i', measured relative to the A_0 sub-array at which these values are zero. From definitions we have:

Table 2. Conversion of sec/deg to km/sec.

sec/deg	km/sec	sec/deg	km/sec
9.00	12.35	11.50	9.67
9.05	12.29	11.55	9.63
9.10	12.22	11.60	9.59
9.15	12.15	11.65	9.54
9.20	12.09	11.70	9.50
9.25	12.02	11.75	9.46
9.30	11.96	11.80	9.42
9.35	11.89	11.85	9.38
9.40	11.83	11.90	9.34
9.45	11.77	11.95	9.30
9.50	11.70	12.00	9.27
9.55	11.64	12.05	9.23
9.60	11.58	12.10	9.19
9.65	11.52	12.15	9.15
9.70	11.46	12.20	9.11
9.75	11.40	12.25	9.08
9.80	11.35	12.30	9.04
9.85	11.29	12.35	9.00
9.90	11.23	12.40	8.97
9.95	11.17	12.45	8.93
10.00	11.12	12.50	8.90
10.05	11.06	12.55	8.86
10.10	11.01	12.60	8.82
10.15	10.95	12.65	8.79
10.20	10.90	12.70	8.76
10.25	10.85	12.75	8.72
10.30	10.80	12.80	8.69
10.35	10.74	12.85	8.65
10.40	10.69	12.90	8.62
10.45	10.64	12.95	8.59
10.50	10.59	13.00	8.55
10.55	10.54	13.05	8.52
10.60	10.49	13.10	8.49
10.65	10.44	13.15	8.46
10.70	10.39	13.20	8.42
10.75	10.34	13.25	8.39
10.80	10.30	13.30	8.36
10.85	10.25	13.35	8.33
10.90	10.20	13.40	8.30
10.95	10.15	13.45	8.27
11.00	10.11	13.50	8.24
11.05	10.06	13.55	8.21
11.10	10.02	13.60	8.18
11.15	9.97	13.65	8.15
11.20	9.93	13.70	8.12
11.25	9.88	13.75	8.09
11.30	9.84	13.80	8.06
11.35	9.80	13.85	8.03

$$X_i = X_i' - 1/M \sum_{k=1}^{M} X_k' \,, \qquad \text{(III. 2)}$$

$$Y_i = Y_i' - 1/M \sum_{k=1}^{M} Y_k' \,, \qquad \text{(III. 3)}$$

and

$$T_i = T_i' - 1/M \sum_{k=1}^{M} T_k' \,, \qquad \text{(III. 4)}$$

where M equals the number of sub-arrays used in the formulation, and i represents an element of the array. We then define a vector $\vec{u}$, sometimes called the slowness vector, which points in the direction of the horizontal component of the seismic ray and has a magnitude equal to the inverse of the horizontal phase velocity. With the following equations in matrix notation,

$$\bar{\bar{A}}\,\vec{u} = \vec{b} \qquad \text{(III. 5)}$$

where

$$\bar{\bar{A}} = \begin{bmatrix} \sum_{i=1}^{M} X_i^2 & \sum_{i=1}^{M} Y_i X_i \\ \sum_{i=1}^{M} X_i Y_i & \sum_{i=1}^{M} Y_i^2 \end{bmatrix} \qquad \text{(III. 6)}$$

$$\vec{b} = \begin{bmatrix} \sum_{i=1}^{M} X_i T_i \\ \sum_{i=1}^{M} Y_i T_i \end{bmatrix} \qquad \text{(III. 7)}$$

and

$$\vec{u} = \begin{bmatrix} u_X \\ u_Y \end{bmatrix} , \qquad \text{(III. 8)}$$

we solve and find:

$$\vec{u} = \bar{\bar{A}}^{-1} \vec{b} \qquad \text{(III. 9)}$$

(see Fairborn, 1968; and Efroymson, 1960). For our root mean square (rms) error, δ , we define ε_i which represents the calculated arrival time for a plane wave at array "i" minus the actual arrival time at that array, T_i. Thus:

$$\sigma = \sqrt{\frac{\sum_{i=1}^{M} \varepsilon_i^2}{M}} \quad . \qquad \text{(III.10)}$$

This method is easily applied to computers to calculate $dt/d\Delta$ from seismic arrays.

For events where first and later arrivals were visible as they crossed LASA, we determined $dt/d\Delta$ from arrivals "picked" from a display scope linked to a PDP-7 computer. Each sub-array trace was aligned visually on the analog display unit, while the digital values were maintained in the computer. From the delay times picked by light pen and the known location of each sub-array, a plane wavefront was fitted by the least squares procedure, and the $dt/d\Delta$, azimuth, and rms error were calculated. Deviations in

measurement of delay time for a good event were .05 seconds. Chinnery and Toksöz (1967); Fairborn (1968); and Scientific Data Laboratory (SDL) Report No. 172 (1966) have reported similar measurement accuracy.

From our data we observed that if an event was picked correctly, then the rms of the time residuals to the best fitting plane wave less than .2 seconds. To the first order approximation this gives a maximum error in $dt/d\Delta$ of .15 sec/deg. For close events (less than $\Delta = 15°$) we tested the plane wave approximation to the wavefront using quadratic surface (see Fairborn, 1968) and found that the two values agreed within the range of normal error, $\pm$ .2 sec/deg.

Events that were recorded on develocorder film had their arrival times picked from prints of the film. These times were then used in the same least squares procedure as described above to find the $dt/d\Delta$, calculated azimuth and rms error. We found the rms error to be at least twice as large as the values for equivalent events recorded on digital magnetic tape.

To assist in picking later arrivals, Calcomp plots were made from digital magnetic tapes of most of the events. These plots were displayed, such that each trace representing a sub-array of LASA was delayed by a time, δT ,

where

$$\delta T = x \cdot (dT/d\Delta). \qquad \text{(III.11a)}$$

Here x equals the radial distance from the event to each sub-array. From these plots, later arrivals could be easily identified and traced as they crossed the array.

In Figure 2 we show several sub-arrays which have been aligned with respect to their real epicenter distance using the previously described technique. This particular event is for $\Delta = 15°$. Notice the later arrival at 10.7 sec/deg. This $dt/d\Delta$ value was consistent with the beams formed for this event. The beam-forming process will be described later in this section.

Most of the variation in the waveform at LASA's sub-arrays appears to be due to multiple paths from LASA's structure and to the different geology at each sub-array (Mack, 1969). Events from the same azimuth and distance have comparable characteristic amplitude variations at each sub-array. Comparison of events from different azimuths shows the variable character of each sub-array, as noted by Sheppard (1967), where we encounter such variables as depth, LASA's inhomogeneity, varied source of functions, and different ray paths due to velocity structure. Our analysis concurs with Mack's (1969) evidence for teleseismic events that LASA seismograms at each sub-array are complicated by the occurrence of multiple paths.

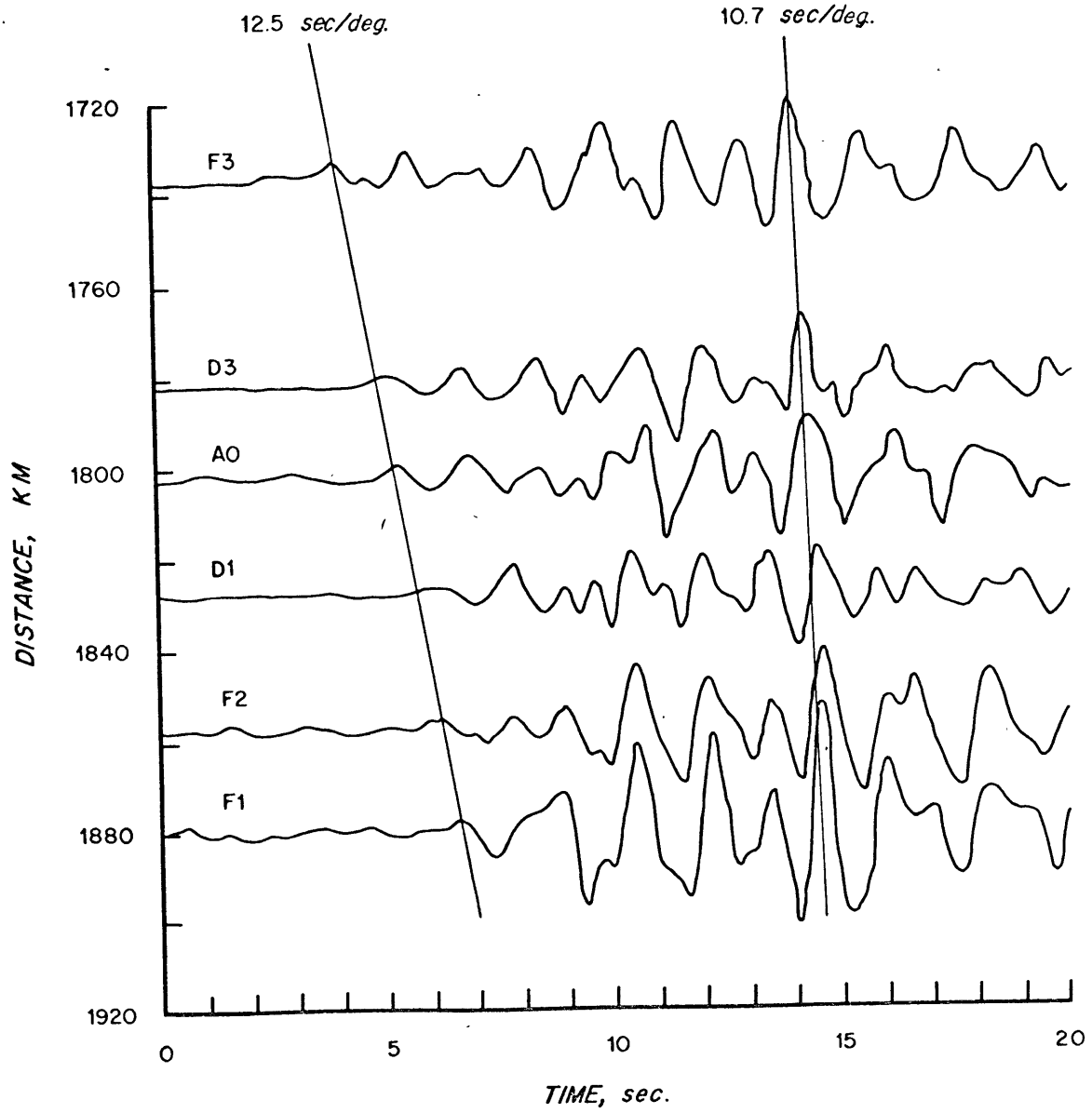

Figure 2. Example of a Calcomp plot for an event which was used to assist picking later arrivals. Note the amplitude difference between the first and later arrival.

To add to the complexity of first and later arrivals, shallow events, which are typical for the region investigated, tend to have a longer and more complicated source function than intermediate and deep events. One way to eliminate the above problems is to form beams with the array. These beams are sensitive to differences in the wave slowness of an incident wavefront and can be used to discriminate between the $dt/d\Delta$ values for later arrivals.

To form beams with LASA, the great circle azimuth and distance are calculated for each sub-array with respect to a given event. The output traces of each sub-array are delayed and summed for progressive values of $dt/d\Delta$. The beams are then displayed, such that the change in wave forms with different $dt/d\Delta$ values could be observed. Later arrivals are then picked from the beams which produced the greatest amplitude, "beam peaks". We used these beams to look for later arrivals that were suspected but not measured, and to verify later arrivals measured from the seismic traces.

To test the efficiency of this method as a criterion for determining $dt/d\Delta$ for later arrivals, beams were formed from synthetic seismograms calculated for LASA, based on the following criteria:

1. The source function would not be significantly different for all arrivals.

2. Multiple paths and delays caused by LASA sub-structure were neglected.
3. Other phases, such as pP, were ignored.
4. Known residuals for various azimuths were added to each sub-array.
5. The possibility of multiple phases was allowed.
6. The travel-times and phase velocities were chosen from Johnson's data (1967).

For our source function we used the first emergent phase at a distance of 40° from the nuclear event, Bilby, which was a simple sinusoidal wavelet. From Johnson's data we allowed three arrivals at 15°. We calculated, using his amplitudes, phase velocities and travel-times, a theoretical seismogram for each sub-array at LASA.

Analysis of the synthetic seismograms generated from the above procedure showed how complex and difficult it would be to pick all arrivals from seismograms, especially at a cross-over. In Figure 3 notice how difficult it is to observe across the entire array the second arrival with the $dt/d\Delta$ of 10.9 sec/deg.

Although this test of our beam-forming procedure as described above is qualitative in nature, it provided several important insights into the analysis of beams for our real data. Using this beam-forming technique, we can show that it is possible to recover the $dt/d\Delta$ of each

Figure 3. Synthetic seismogram showing the arrival of three phases.

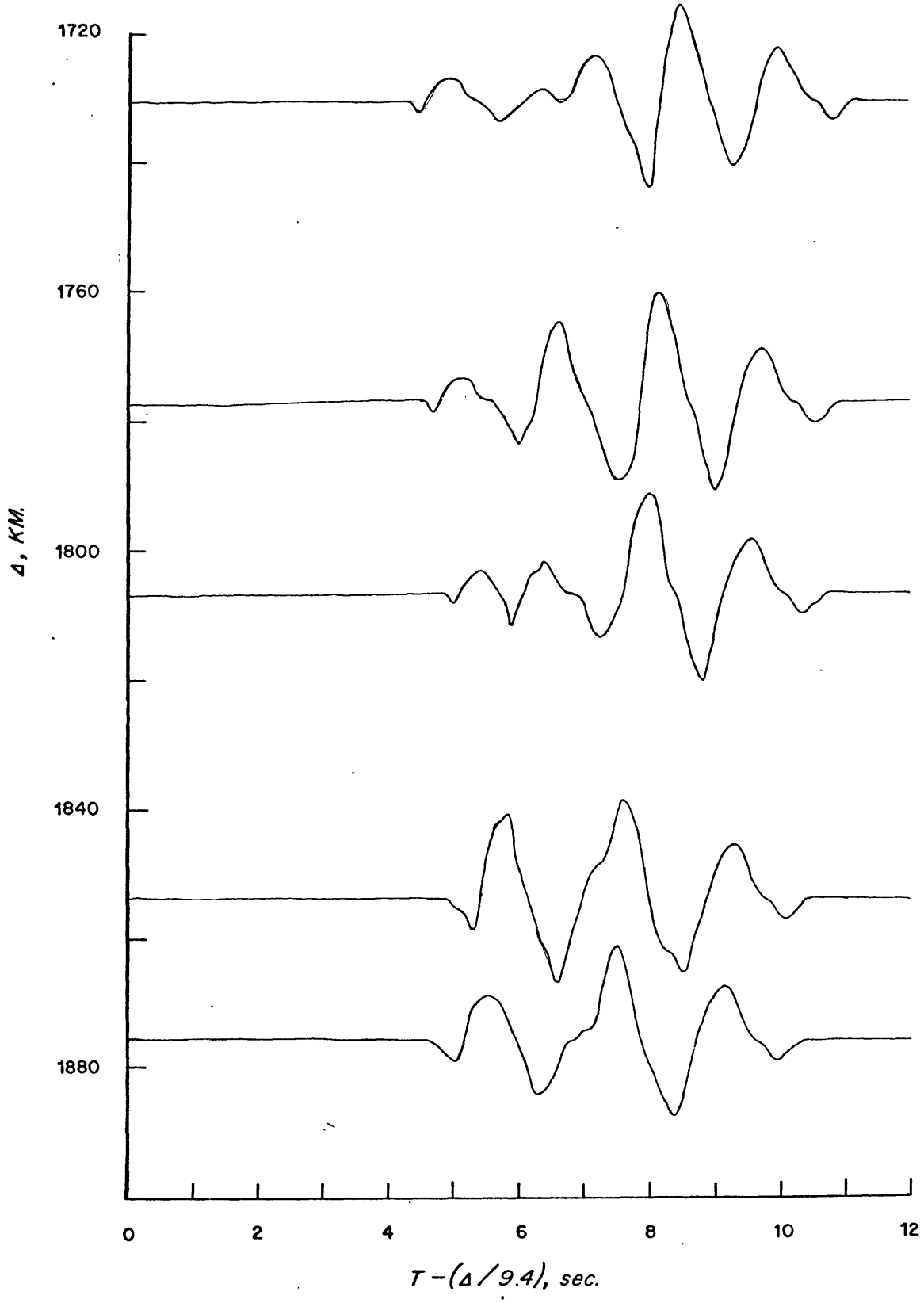

arrival ± .2 sec/deg. Addition of known time residuals for each sub-array does not significantly alter the "beam peaks". Difficulties that we encountered were that smaller arrivals tended to be "masked" by the larger arrivals, and that amplitude differences between arrivals were only crudely recoverable, due to "lobes" and later arrivals being in and out of phase.

Another peculiarity observed from these beams was that a "peak", representing the input $dt/d\Delta$ value, develops faster on the side of the next incoming wave. For example, for a series of beams, if 8.0 sec/deg represents the inverse phase velocity of an incoming wave, and 7.0 is the next incoming wave, then the 7.5 beam is larger than the 8.5 beam.

In Figure 4, we show beams formed from the synthetic seismograms, where we have added the characteristic time residuals for this distance and azimuth. We have attempted to measure the $dt/d\Delta$ values of 13.0, 9.90, and 11.6 sec/deg. We demonstrate here that we are able to recover these values with an accuracy of ± .2 sec/deg. Notice the "skewness" characteristic of the beams as described previously.

In Figure 5 we show beams formed from real data with different values of $dt/d\Delta$. Observe the peaks at 10.86, 10.07, and 9.56. One can see various waveforms

Figure 4. Beams formed with LASA with synthetic seismograms.

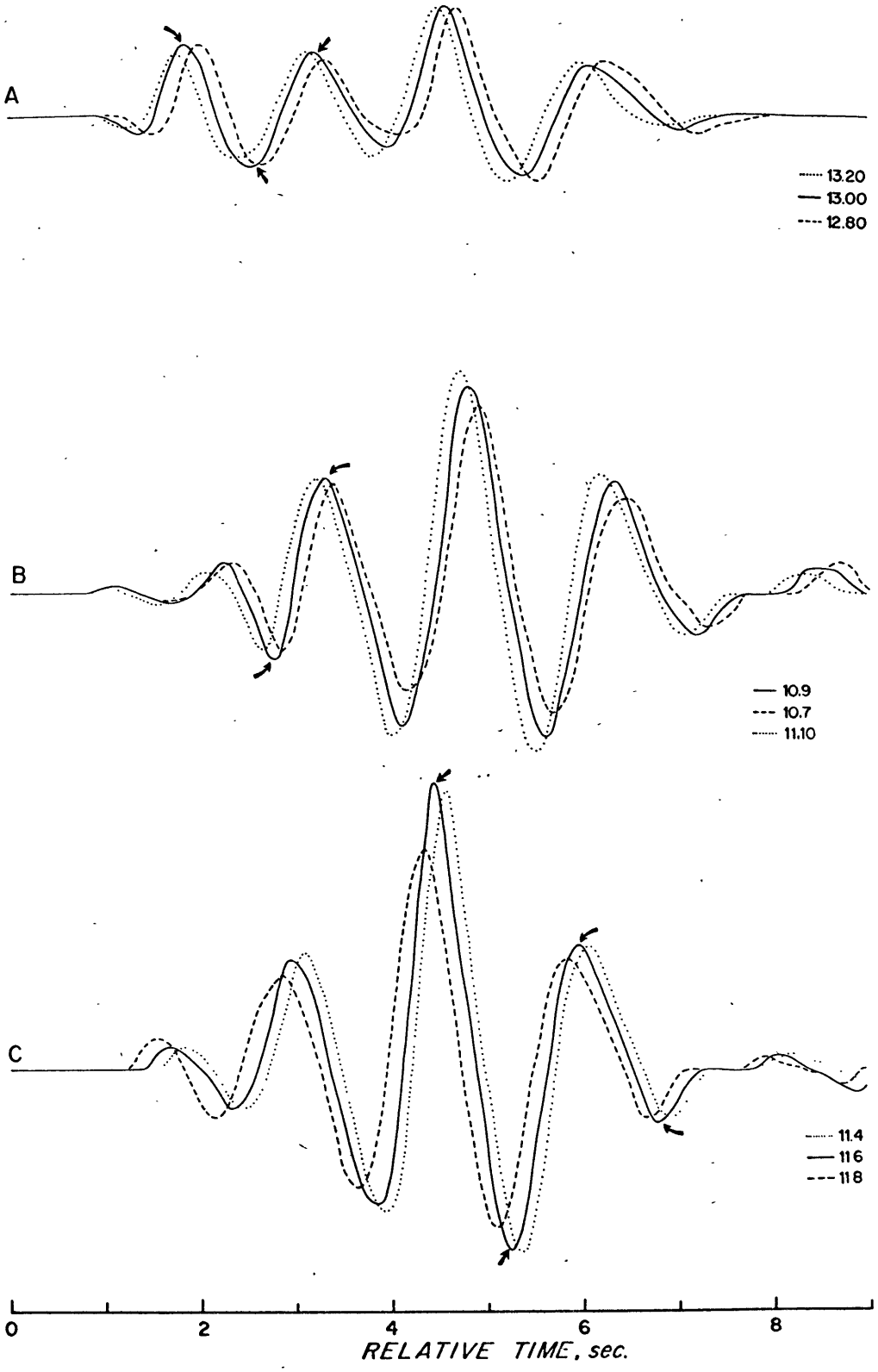

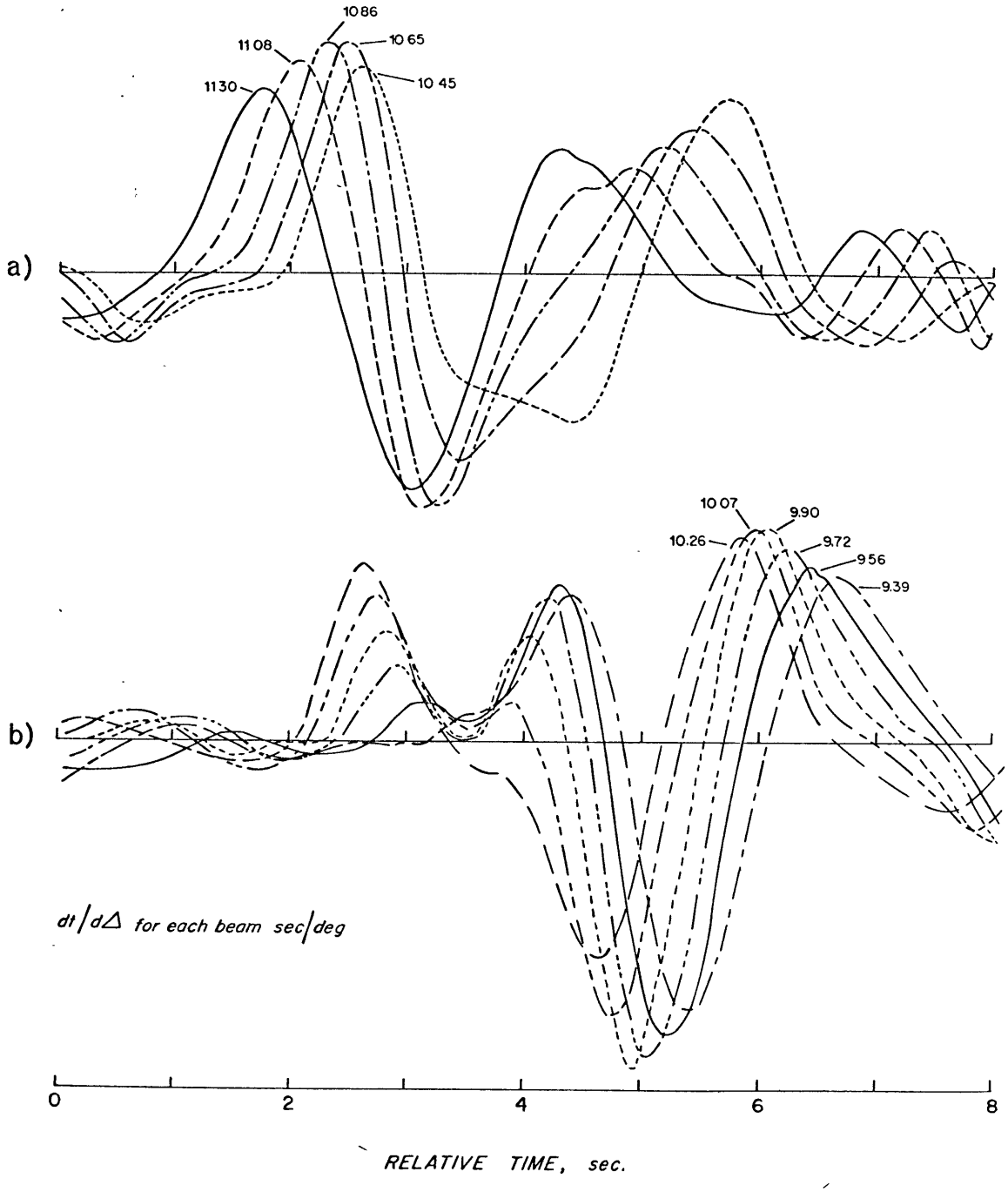

Figure 5. Real beams formed with LASA from event number 40.

developing as the later arrivals come into phase. Notice again how the peaks are skewed to the closest waveform, as noted in the synthetic beams.

Along with measuring $dt/d\Delta$ values, we also looked at the travel-times for our events. Unfortunately, the distribution of these events was not good enough to do a statistical averaging for determining absolute travel-time after removing epicenter and timing errors. However, Fairborn (1968) noted for the LASA that the scatter in travel-time was ± 2 seconds, and that there were no observable travel-times associated with any particular source region which appeared anomalous. This data concurs with Lincoln Laboratory Report No. LL-6. Therefore, we used the travel-times given by Herrin, et al. (1968), and Julian and Anderson (1968) as constraints for the Monte Carlo inversion program of Wiggins (1969). These travel-times were consistent with our measurements and were derived from data from North America.

For our plane wave residuals (defined as: calculated arrival time minus the observed arrival time), we found very good correlation between events at the same distance and azimuth, lesser correlation for events at different distances, and no correlation for events at different azimuths regardless of distance. We have not included our data for this observation. A more comprehensive investi-

gation was made by Sheppard (1967) for teleseismic events. The above observations apparently indicate that the structure causing the travel-time anomalies is deep enough, such that it is not sampled from ray paths of different azimuths or the structure is very sharp causing rays arriving from different angles to be diffracted with a time delay.

Sheppard (1967) found that when he plotted his station correction (defined as: the correction necessary for the various sub-arrays to make the measured value of phase velocity equal the real value), the anomalies indicate a syncline-shaped structure trending in a northeasterly direction passing through the center of LASA. We have looked at the time-residuals from a plane wave approximation of several PKP events that had a phase velocity greater than 180 km/sec. These residuals had the general character of Sheppard's indicated time-residual structure. In an effort to locate the cause of these residuals, we plotted several parameters, such as Bouguer gravity, amplitude, travel-time residual, azimuth, and azimuth deviation (defined as: true azimuth minus calculated azimuth) for each sub-array. We concluded that there is a correlation between time delay and amplitude for a nearly perpendicular wave-front. We also found that there existed no visible correlation between amplitudes and travel-times with

respect to different distances and azimuths for all the LASA sub-arrays. This fact was in agreement with the Lincoln Laboratory report no. LL-3, which used teleseismic data. Finally, we found Bouguer gravity appears to be unrelated to amplitude and travel-time delays. These correlations were useful for indicating the general structure under LASA, but could not define the exact geometry.

We have dealt with amplitude variation in a qualitative nature due to the large variability of amplitude with azimuth and distance at LASA, (Lincoln Laboratory report no. LL-3). The works of Romney, et al. (1959); Lehmann (1964); Wright, et al. (1966); Johnson (1967); Lewis and Meyer (1968); and Kanamori (1967) generally agree as to the typical pattern of amplitude behavior up to $\Delta = 30°$. This behavior is as follows: a decrease in amplitude of P_n to 11-13° crossing over to another arrival at p = 13.0 sec/deg. The next first arrival, 10.6 sec/deg, starts at $\Delta = 18°$ and decreases in amplitude as a first arrival until it becomes a later arrival at $\Delta = 24°$, where the emergent phase has a $dt/d\Delta$ of 9.0 sec/deg. We can see that this amplitude behavior is typified by emergent phases of low amplitude at 11-13°, 18-19°, and 23-24°. However, the amplitude is always larger than the previous first arrival and decays until the next crossover. Later arrivals which have been identified are invariably of larger amplitude and

can be seen from 9-27°.

The above observations are generally consistent with our data. We observed at 9° an arrival with an uncorrected $dt/d\Delta$ of 13.5 sec/deg. For the event shown in Figure 6, we noticed that there existed a later arrival that had a much larger amplitude and arrived about 5 seconds. However, this arrival had the same $dt/d\Delta$ as the first arrival. Since there existed only one event for this region we could not verify whether this arrival was a peculiarity of the source function or a bona fide refraction from a lower layer. Near the 17° cross-over, we measured a $dt/d\Delta$ of 12.9 sec/deg for the first arrival and 12.00 sec/deg for a later arrival. In Figure 7, we show the greater amplitude of the later arrival and the difficulty in identifying the first arrival. At the 20° discontinuity we found a first arrival with the $dt/d\Delta$ of 11.2 sec/deg which was followed by a later arrival with a larger amplitude and a $dt/d\Delta$ of 12.4 sec/deg. This later arrival is probably related to the 11.95 sec/deg arrival at 17°. Before the 24° cross-over we found the first arrival to have a $dt/d\Delta$ of 10.7 sec/deg. This arrival was followed by later arrivals with $dt/d\Delta$ values of 12.9 and 9.6 sec/deg. After the 24° cross-over we measured a second arrival with a $dt/d\Delta$ of 9.8 sec/deg and a smaller first arrival with a $dt/d\Delta$ of 9.1 sec/deg. The first arrival decreased in $dt/d\Delta$ to 8.95

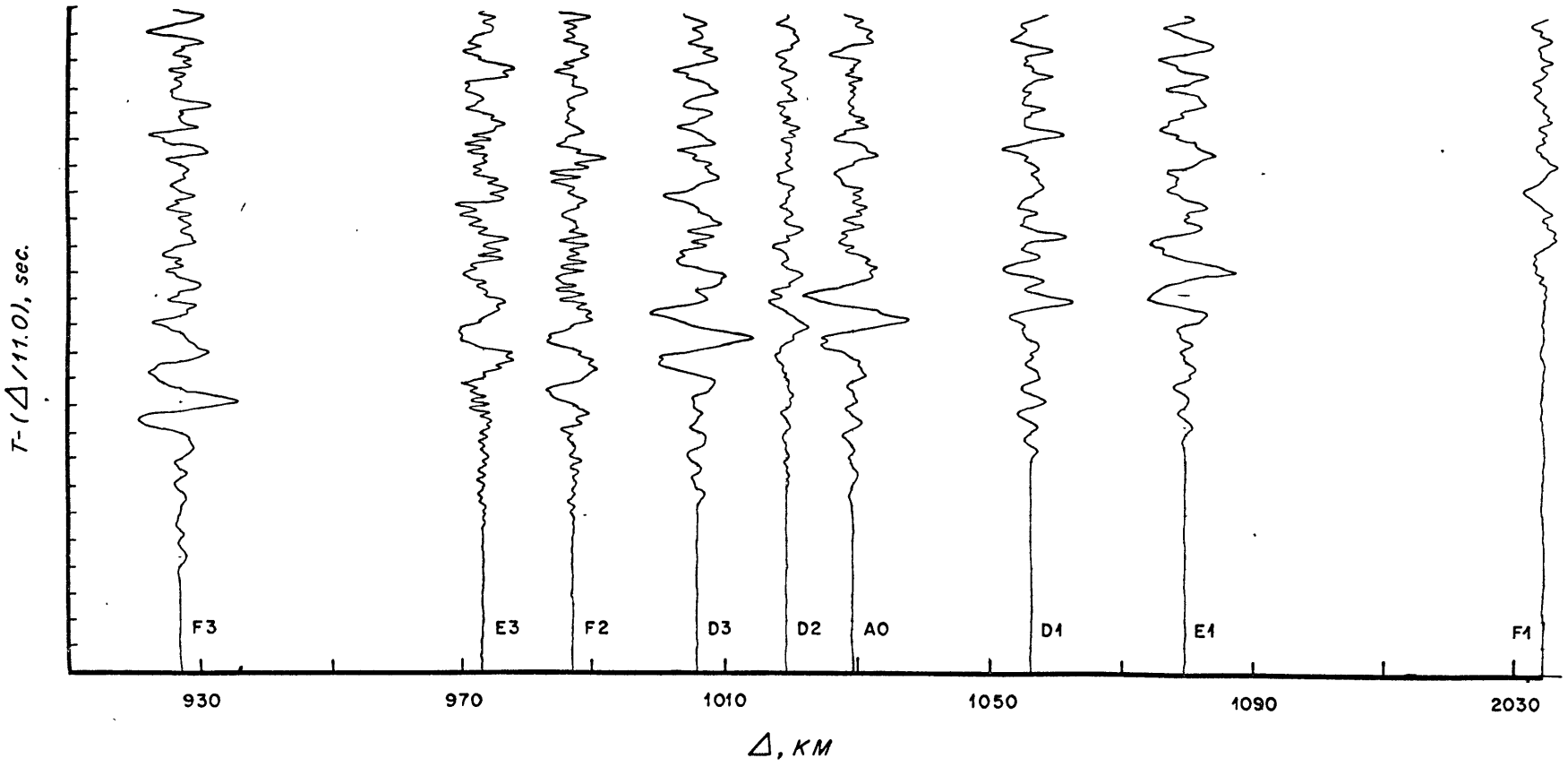

Figure 6. Calcomp plot of event number 21 showing two arrivals with the same phase velocity.

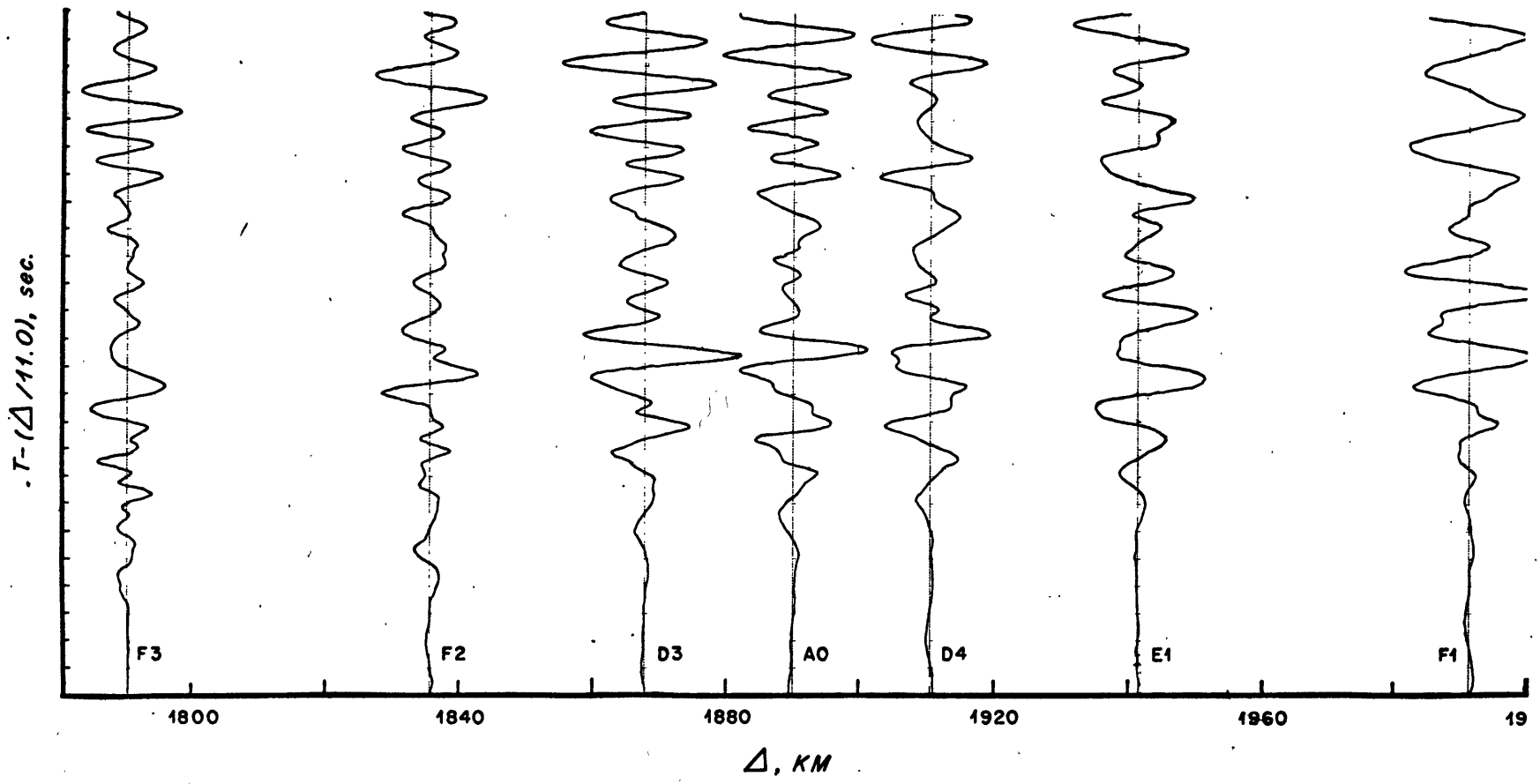

Figure 7. Calcomp plot of event number 40 showing two arrivals with different phase velocities.

sec/deg at 30 degrees while the second arrival decreased in amplitude and was not observable past 27°.

From our initial $dt/d\Delta$ data, Table 3, we have identified an azimuthal dependence of $dt/d\Delta$ (Figure 8), which was also observed by Fairborn (1968), Toksöz, et al. (1967), and Greenfield and Sheppard (1969). The cause for these azimuthal variations in $dt/d\Delta$ could be an effect of LASA substructure or different velocity profiles for the northwest and south azimuths (or both).

Fairborn (1968), in his correction for LASA structure, chose to throw out values of $dt/d\Delta$ for $\Delta = 28°$ to $40°$ in the southern azimuth because of the irreconcilability of the "travel-time residuals". This fact indicates that at near teleseismic distances LASA's structural anomalies are still affecting the measured wave slowness. Therefore, the "grid correction" approach which he uses is probably not applicable to this study. Nonetheless, we tried his approach and found that our earthquake distribution was skewed and that the number of good events was too few to develop any reasonable grid residuals. However, Fairborn observed that there is a minimum in time residuals for a plane wave at 40 km and 20 km, and he subjectively suggests that the structural inhomogeneity may extend into the upper mantle.

Greenfield and Sheppard (1969) have proposed a model

Table 3. dt/dΔ Measurements * +

EVENT NO.	DISTANCE DEGREE	DEPTH KM	CORRECTED DISTANCE	OBSERVED P	CORRECTED P	RMS ERROR
1	20.18	34	20.33	11.25	10.89	.18
				12.40	12.04	.11
2	29.76	54	30.11	9.39	8.98	.21
3	15.36	33	15.36	12.77	12.60	.33
				12.25	12.08	.37
				11.30	11.13	.30
				13.18	13.01	
				12.57	12.40	
				11.50	11.33	
				10.18	10.01	
4	15.23	33	15.23	13.21	13.04	.46
				11.61	11.44	.32
				11.13	10.96	
				10.18	10.01	
				12.46	12.29	
5	26.97	38	27.07	8.94	8.93	.09
6	28.55	86	29.11	9.41	9.00	.15
7	29.53	62	29.93	9.31	8.90	.16
8	16.48	6	16.31	12.29	12.24	.23
				11.10	11.05	.30
				12.58	12.53	.29
				12.46	12.41	
				11.68	11.63	
9	28.80	102	29.46	8.89	8.86	.14
10	29.19	32	29.19	8.92	8.92	.14
11	28.71	97	29.31	9.63	9.22	.33
12	30.98	33	30.98	8.87	8.87	.14
13	6.88	5	6.63	13.71	13.29	
14	15.95	33	15.95	12.13	12.07	
				11.39	11.33	
15	15.02	10	15.02	11.44	11.21	
				10.99	10.76	
16	26.93	33	26.93	9.50	9.13	.12
				9.24	8.87	
				10.26	9.89	
17	31.07	45	31.32	9.33	8.95	.18
18	16.71	33	16.71	11.61	11.29	.11
19	17.18	33	17.18	13.09	12.79	.12
				11.57	11.27	.19
20	27.21	28	27.21	8.99	8.98	.13
21	9.26	18	9.11	13.46	13.16	.16
22	21.81	33	21.81	10.45	10.44	.20
				9.35	9.34	.14
23	26.13	33	26.13	9.06	9.05	.11
				9.72	9.71	.14

* Values without rms error represent dt/dΔ from beams.
\+ Events 62--92 are from develcorder films.

Table 3, Continued

EVENT NO.	DISTANCE DEGREE	DEPTH KM	CORRECTED DISTANCE	OBSERVED P	CORRECTED P	RMS ERROR
				9.15	9.14	
				9.62	9.61	
24	24.32	16	24.21	9.02	9.00	.16
				9.76	9.74	.18
25	6.78	5	6.51	13.90	13.48	.41
26	22.67	33	22.67	10.74	10.36	.20
				9.95	9.57	.11
				12.87	12.49	
				10.65	10.27	
				11.30	10.92	
				9.72	9.34	
27	15.22	33	15.22	10.79	10.66	.25
28	17.00	33	17.00	12.88	12.56	.25
				11.95	11.63	.17
29	16.97	33	16.97	12.73	12.41	.23
				12.03	11.71	.16
30	14.93	15	14.93	10.60	10.43	
				11.80	11.63	
31	15.09	11	14.94	11.31	11.08	.19
				12.14	11.91	.42
				13.36	13.13	
				11.21	10.98	
32	10.01	0	10.01	13.82	13.44	.20
33	16.03	33	16.03	12.47	12.35	.18
				13.69	13.57	
				10.77	10.65	
				12.19	12.07	
34	16.17	33	16.17	12.48	12.36	.17
				10.74	10.62	.19
				13.05	12.93	
				10.99	10.87	
				12.46	12.34	
35	16.10	33	16.10	12.47	12.35	.21
				13.69	13.57	
				10.99	10.87	
				12.56	12.44	
36	14.48	33	14.48	13.05	12.87	
				11.75	11.57	
				10.99	10.81	
37	27.09	19	27.03	8.97	8.96	.11
38	10.51	0	10.51	13.26	13.01	.15
39	14.77	33	14.77	10.57	10.43	.10
				13.52	13.38	.41
				13.69	13.55	
				13.05	12.91	

Table 3, Continued

EVENT NO.	DISTANCE DEGREE	DEPTH KM	CORRECTED DISTANCE	OBSERVED P	CORRECTED P	RMS ERROR
				11.93	11.79	
40	22.74	.33	22.74	10.69	10.34	.33
				12.87	12.52	
				10.86	10.51	
				9.56	9.21	
				10.07	9.72	
41	9.87	18	9.77	12.65	12.43	.13
				13.50	13.28	
				13.05	12.83	
				10.77	10.55	
42	16.01	14	15.84	12.47	12.41	.21
				12.28	12.22	.17
				13.29	13.23	
				12.40	12.34	
				10.33	10.27	
43	28.84	25	28.84	9.00	8.90	
44	30.44	9	30.34	9.36	8.95	.17
45	24.80	33	24.80	9.04	9.02	
				9.84	9.82	
				10.39	10.37	
				9.67	9.65	
46	15.53	33	15.53	12.71	12.64	.24
47	14.27	8	14.27	12.60	12.37	
				11.40	11.17	
				13.05	12.82	
				13.69	13.46	
				12.46	12.23	
48	15.53	20	15.42	13.30	13.01	.12
				13.40	13.11	
				11.60	11.31	
49	15.40	15	15.40	12.40	12.11	
				11.60	11.31	
				10.40	10.11	
50	28.58	23	28.63	8.95	8.95	.12
51	12.00	0	12.20	13.25	12.98	.16
52	17.43	0	17.17	12.44	12.30	.22
53	27.43	28	27.43	8.95	8.93	.11
54	9.88	33	9.88	13.12	12.91	.22
55	27.92	33	27.92	9.39	9.00	.10
56	30.83	40	31.03	9.48	9.08	.12
57	31.31	33	31.31	9.27	8.87	.19
58	12.00	0	12.25	13.28	13.00	.16
59	13.69	0	13.69	11.13	10.99	.28
60	15.74	19	15.64	12.80	12.54	.26
61	26.44	0	26.44	9.52	9.15	.13

Table 3, Continued

EVENT NO.	DISTANCE DEGREE	DEPTH KM	CORRECTED DISTANCE	OBSERVED P	CORRECTED P	RMS ERROR
				0.00	-0.37	
62	12.00	0	12.25	13.25	12.98	.15
63	29.60	33	29.60	9.33	9.32	.28
64	14.80	33	14.80	12.59	12.43	.15
65	28.40	72	28.87	9.43	9.02	.13
66	30.40	33	30.40	8.99	8.98	.08
67	27.80	54	28.11	9.62	9.23	.15
68	12.00	0	12.25	13.62	13.36	.09
69	21.80	33	21.80	10.81	10.44	.09
70	16.00	37	16.00	12.89	12.83	.43
71	25.50	53	25.52	9.58	9.20	.10
72	25.60	48	25.62	9.65	9.27	.28
73	25.30	58	25.33	9.48	9.10	.18
74	12.00	0	11.60	14.13	13.86	.30
75	34.00	87	34.00	9.07	8.69	.21
76	27.80	53	28.09	9.01	8.99	.12
77	12.00	0	12.25	13.12	12.86	.21
78	15.40	18	15.29	13.47	13.34	.26
79	28.30	33	28.30	8.98	8.96	.15
80	16.20	33	16.20	13.08	12.77	.27
81	11.00	33	11.00	14.00	13.71	.30
82	13.10	0	13.10	13.35	13.21	.29
83	6.90	5	6.63	13.79	13.45	.17
84	14.70	0	14.70	13.85	13.56	.19
85	21.20	33	21.20	11.05	10.68	.16
86	17.30	33	17.30	10.42	10.39	.27
87	16.50	6	16.30	11.90	11.85	.30
88	15.30	33	15.30	10.69	10.56	.25
89	13.00	0	13.00	13.41	13.13	.24
90	21.90	0	21.90	10.59	10.23	.20
91	6.90	5	6.50	14.00	13.58	.23
92	15.00	33	15.00	12.54	12.40	.24

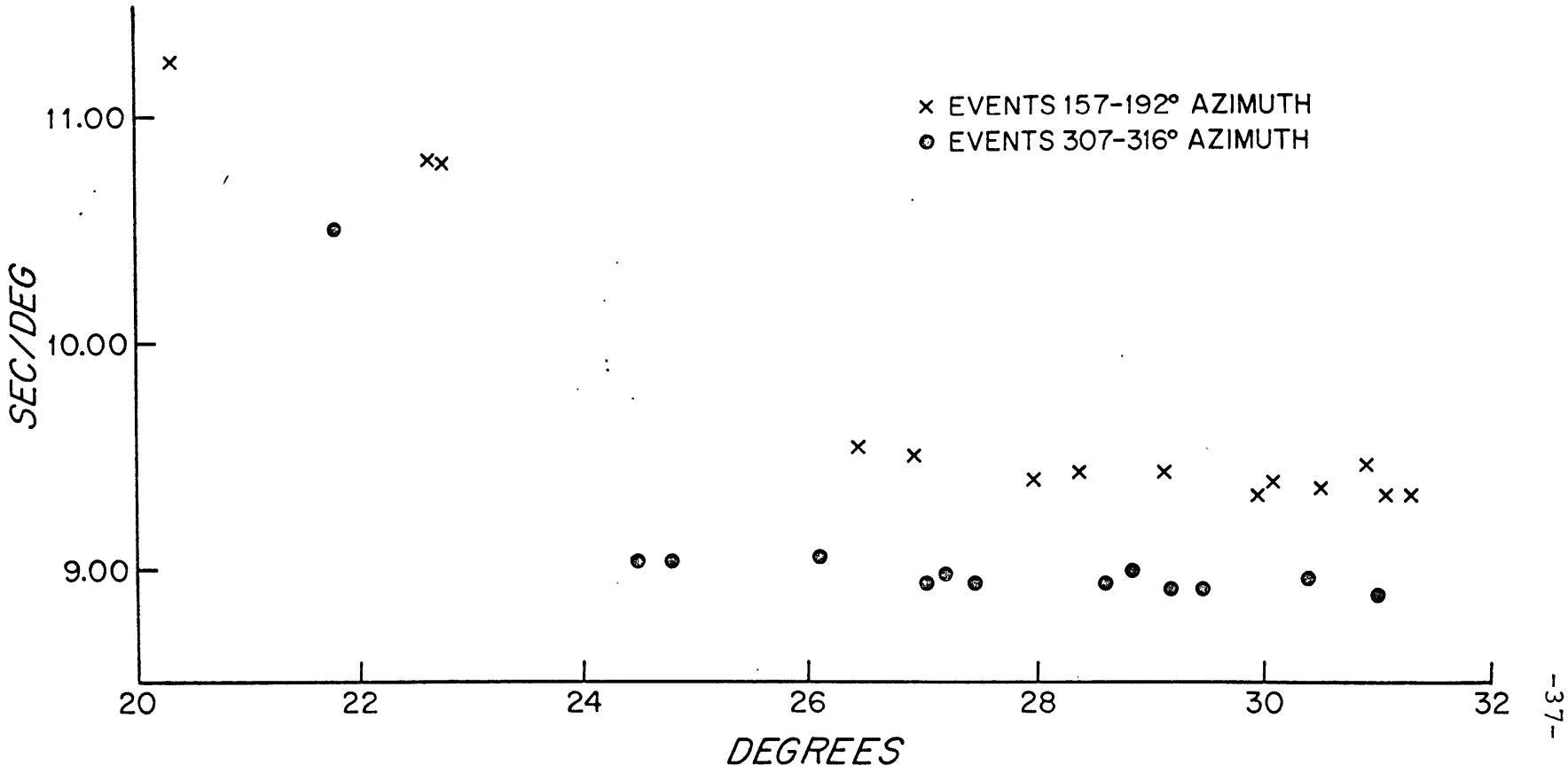

Figure 8. Uncorrected values of dt/dΔ showing the azimuthal dependents.

for LASA. The model was developed to bring the teleseismic data available from the northwest and south azimuths into accord. The structure that they proposed is linear, trending in the N 60 E direction (see Figure 9), and consists of several dipping layers with a velocity contrast of 6.0 and 8.0 km/sec, for the crust and upper mantle respectively. They set this boundary at approximately 60 km. One should note that this model does not satisfy the observed Bouguer gravity anomaly (Figure 9). Another feature of this model is that the structure is deeper than Fairborn's "grid residuals" predict.

We generated hypothetical time residuals and azimuth variations for $dt/d\Delta$ values from 14.0 to 9.0 sec/deg (8.00 to 12.35 km/sec) for various azimuths, using Greenfield and Sheppard's (1969) program for their structural model. The outcome of the above calculation shows that their predicted azimuth variation and the actual variation have very limited correspondence (Figure 10a). Also, the model does not bring the measured phase velocity into any coherence from the various azimuths. This fact was especially true of $dt/d\Delta$ measured at $\Delta = 22°$ (10.5 and 10.75 sec/deg for the northwest, 310°, and south, 185°, azimuths respectively), where we receive a refracted wave from the 350 km discontinuity. Here, using the Greenfield and Sheppard's model, we calculated $dt/d\Delta$ deviations for these

Figure 9. Greenfield and Sheppard's structure for LASA and the associated Bouguer gravity.

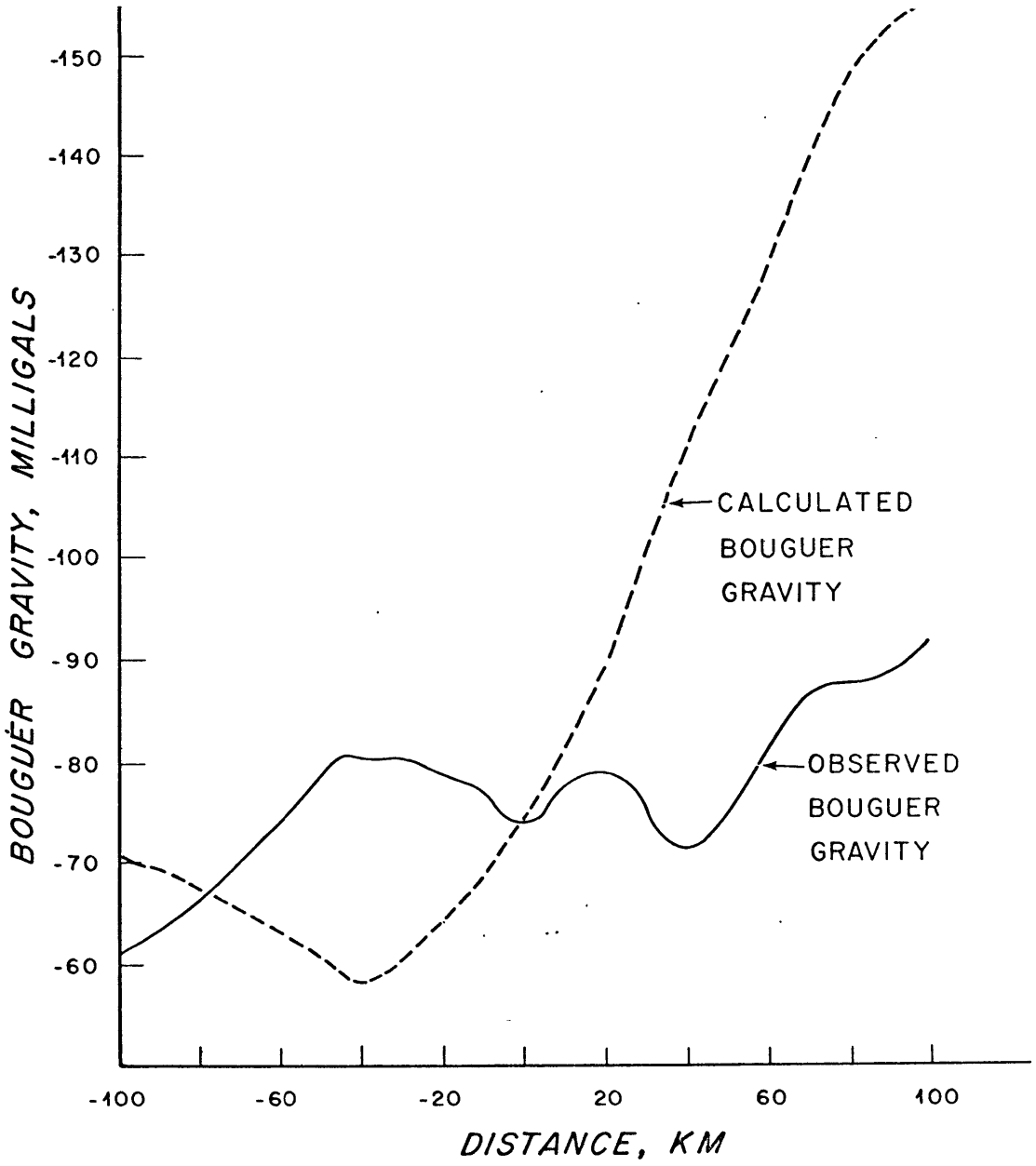

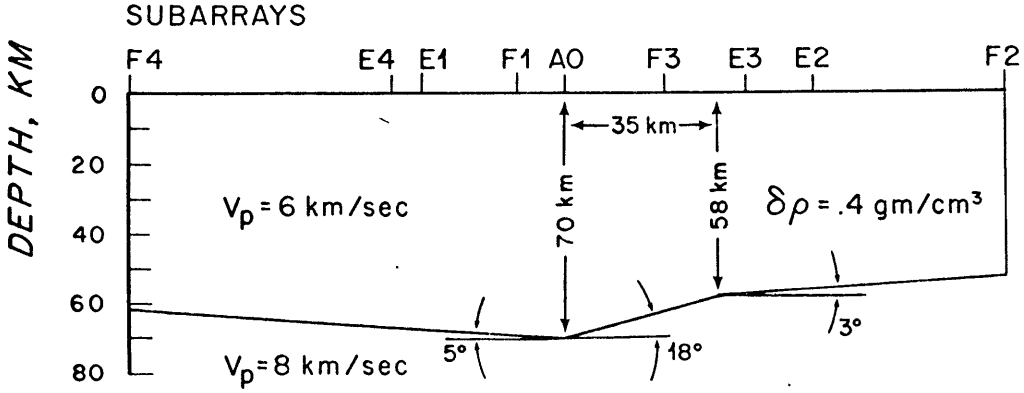

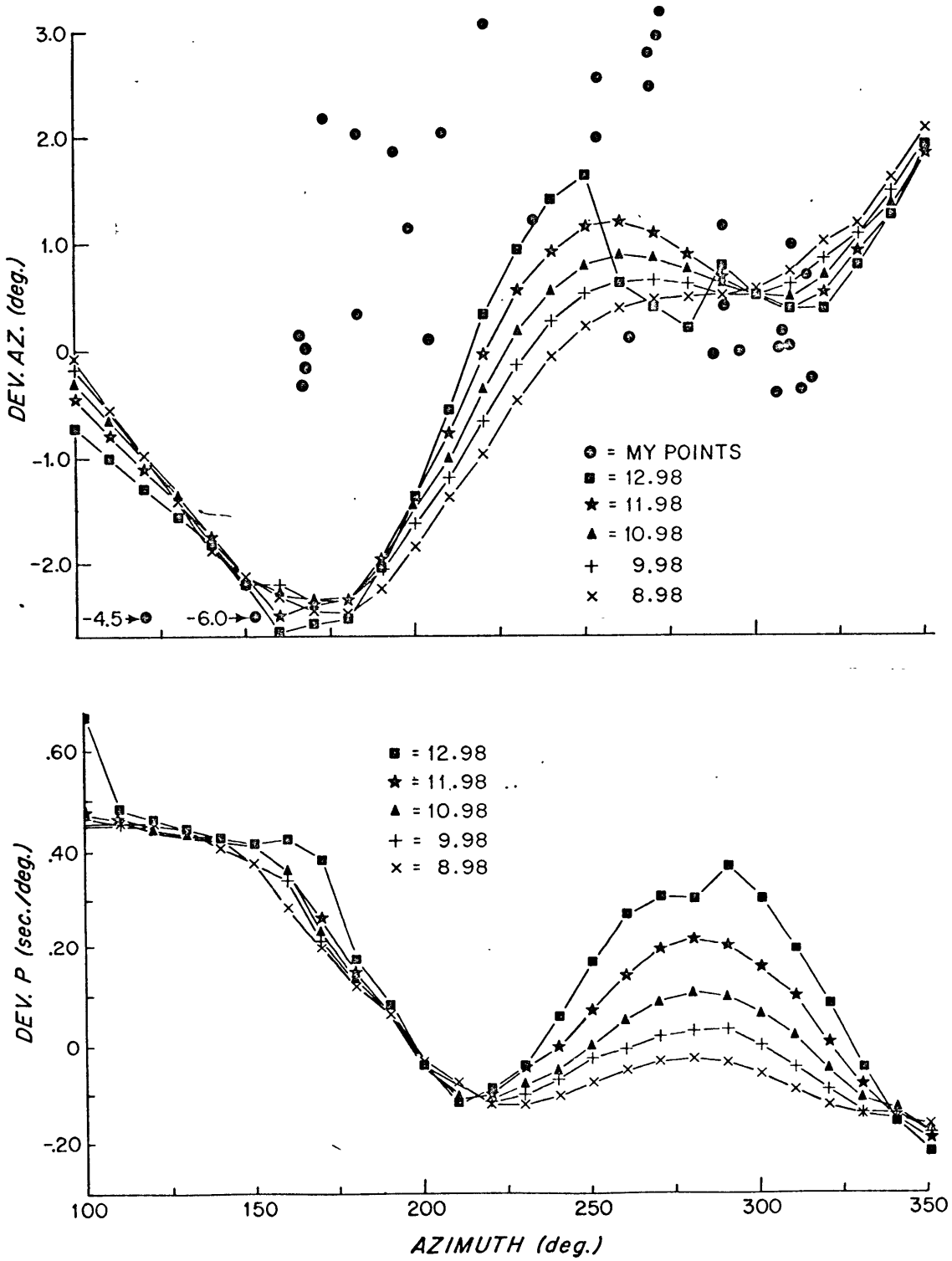

Figure 10. Calculated azimuthal deviation and plane wave deviation for Greenfield and Sheppard's LASA model.

azimuths to be less than .05 sec/deg, as compared to the actual deviations of .25 sec/deg (Figure 10b).

We concluded that no existing models for LASA's substructure would be appropriate for $dt/d\Delta$ azimuthal correction for short ($\Delta < 24°$) epicentral distances. However, it appears that the azimuthal variations are reconcilable, if we look first at the data of other investigators, and then attempt to align our results with theirs. Johnson's (1967) data from the Tonto Forest Array in Arizona, and Chinnery and Toksöz's (1967) data from LASA indicate that the 9.0 sec/deg, which has ray paths bottoming under the Northern Rockies is a representative value for the 650 km discontinuity for our northwest azimuth. The 9.45 sec/deg value that we measured for the southern azimuth should correspond to the value obtained by Johnson's (1967) 9.00 sec/deg, since the sampled area is approximately the same.

The above suggests that the 9.45 value should be adjusted to 9.00 sec/deg. In the absence of any other evidence, and since the other investigators corroborate the 9.0 sec/deg value for the 650 km discontinuity, we have assumed that the apparent azimuthal velocity anisotropy is a result of LASA's substructure. It can be shown that through either peculiar layering (Greenfield and Sheppard, 1969) or rock anisotropy (Crosson and Christensen, 1969; and Christensen and Crosson, 1967) that such conditions can

exist. Therefore, we corrected our measured values of $dt/d\Delta$ for azimuth (A), using:

$$dt/d\Delta = .003 \mid 310°-A \mid \qquad \text{(III.12)}$$

$$\text{where } A = \begin{cases} 340-A & \text{for } 0<A<170 \qquad \text{(III.13a)} \\ A & \text{for } 170<A<360 \qquad \text{(III.13b)} \end{cases}$$

We derived this particular algorithm, such that the refracted waves from the 650 km discontinuity, from the different azimuths 160° and 340°, were in accord. This correction lowered the scatter of the $dt/d\Delta$ measurements over most distances, as seen in Figure 11, lending some credibility to this approximation. The adjusted values are listed with the uncorrected measurements in Table 3.

Inversion of our data was done by putting appropriate limits on the acceptable values of $dt/d\Delta$ rather than by forcing a curve through our measured values of $dt/d\Delta$ versus distance. We also included Johnson's (1967) data, noting that his data enhanced ours where we lacked data due to seismicity. With the use of the Monte Carlo method of Wiggins (1969), we generated random velocity models that were acceptable to our travel-time and $dt/d\Delta$ constraints. Figure 12 is a composite of all the acceptable velocity models. The corresponding $dt/d\Delta$ curves for these models are plotted in Figure 11.

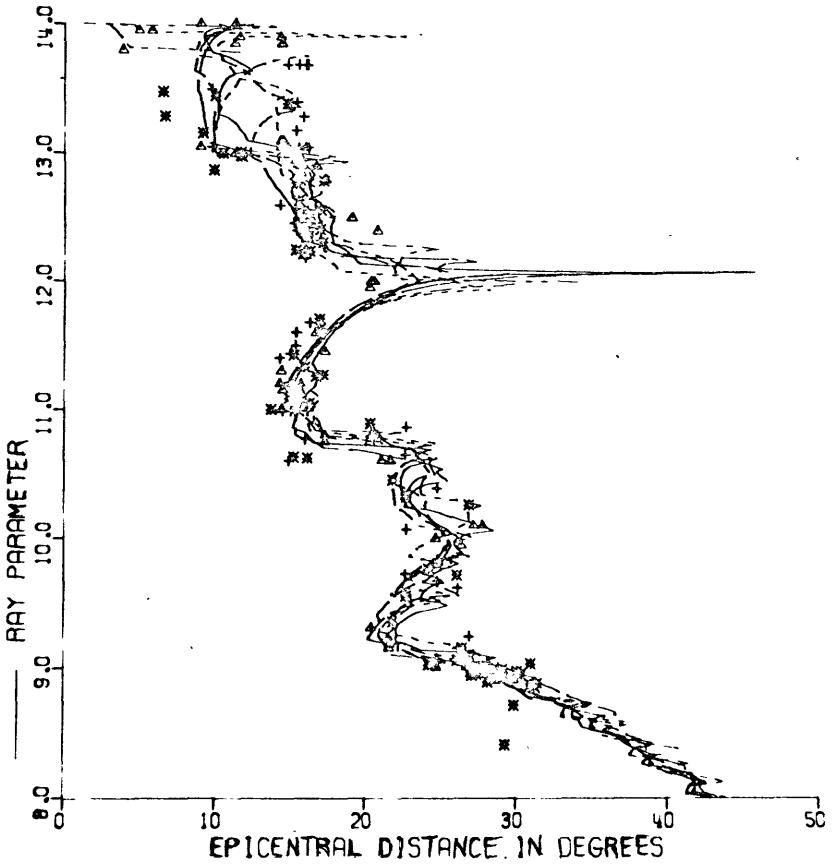

Figure 11. dt/dΔ measurements. The stars (*) are dt/dΔ calculated from LASA arrival times, the plus marks (+) are values from beams formed with LASA, and the deltas (Δ) are Johnson's (1967) data.

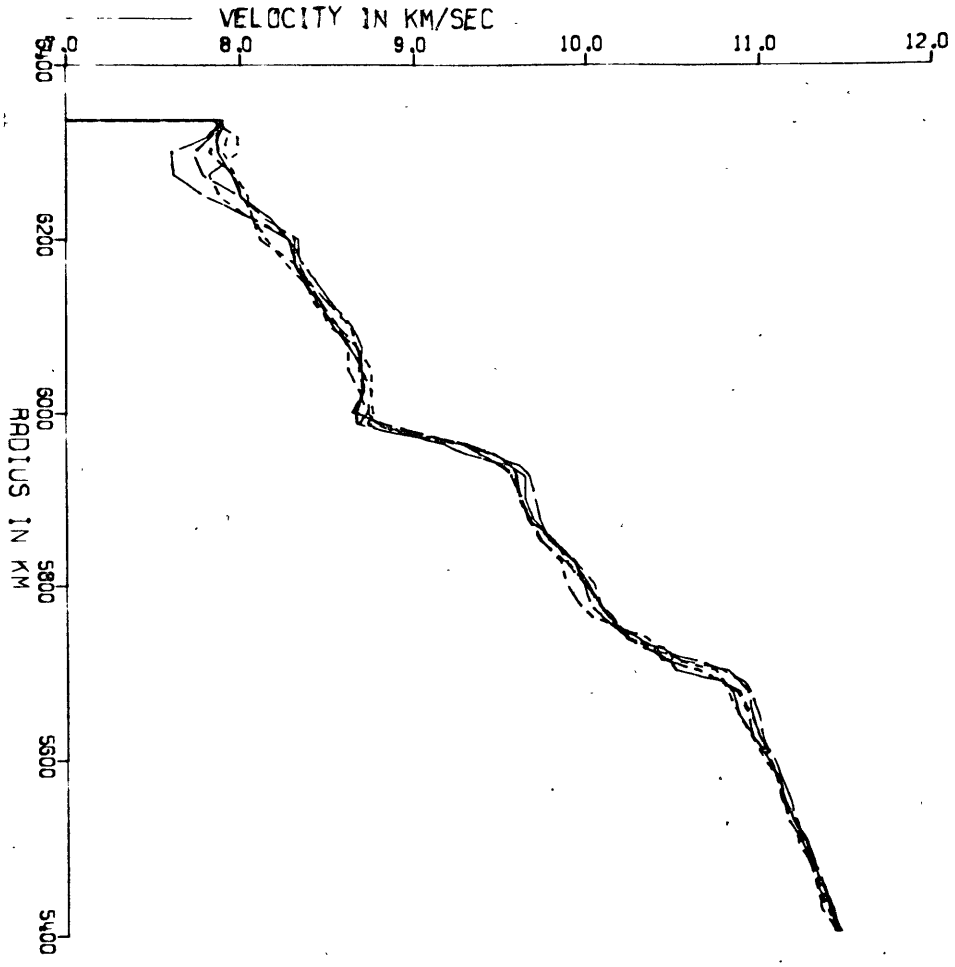

Figure 12. Velocity structures derived from the Monte Carlo method.

In Figure 12 we can see the high variability of the velocity structure in the upper 150 km of the upper mantle. This is a region where reception of refracted waves may go undetected because of their low amplitude. This portion of the upper mantle appears to have a highly variable velocity structure from region to region (Herrin and Taggart, 1962). This undetectability of waves and variability of wave velocity in addition to an indeterminate structure beneath LASA contributes to the scatter in our $dt/d\Delta$ data. Consequently, we have many different, but acceptable, velocity models, most with a low velocity zone, for the 100 km region.

All of our models converge around 150 km with the approximate velocity of 8.3 km/sec. Our models have two zones of rapid velocity increase at 350 and 650 km, as was found by other investigators for western North America (Johnson, 1967; Green and Hales, 1968; and Julian and Anderson, 1968). General features of our models is a steady increase in velocity from 8.3 km/sec (150 km) to 8.7 km/sec (250 km). At 250 km depth the velocity does not increase as rapidly with depth until 300 km where it increases to 9.6 km/sec at a depth of 350 km. At 350 km the upper mantle then appears slowly to increase in velocity until 560 km where the compressional velocity is 10.2 km/sec. Here the velocity increases to 10.9 km/sec at a depth of 650 km. In Figure 12, one can see the possible existence

of small low velocity zones before and after each velocity discontinuity. With the accuracy of the available data their presence cannot be proved or disproved.

IV. CONCLUSION

We have shown that $dt/d\Delta$ can be measured reliably for first and later arrivals using LASA. If later arrivals are observable across the array, we can calculate $dt/d\Delta$ for them with nearly the same accuracy as the first arrivals. Our procedure for picking later arrivals has been aided by the use of Calcomp plots of the seismic trace at each array aligned with the incoming wave front. Also, we have demonstrated that with beams formed with LASA it is possible to recover $dt/d\Delta$ values within $\pm$ .2 sec/deg for $dt/d\Delta$ greater than 9.0 sec/deg. The advantage of using the beam-forming method is that we have been able to obtain apparent phase velocity measurements from complex data that had low amplitude later arrivals. In addition, this method enabled us to verify arrivals that were suspected but too marginal to measure.

Inversion of our $dt/d\Delta$ data shows our compressional velocity models for the upper mantle to be consistent with the model of Johnson (1967) with only variations in some of the details. Most of our models support the supposed low velocity zone at approximately 100 km depth. However, due to seismicity, to a too low recording interval at LASA (0.05 sec), and to the high variability of P_n (and therefore MOHO structure in Western North America), we cannot decisively conclude that the low velocity zone exists.

We have, as the other investigators have, defined two zones of rapid velocity increase with depth, one at 350 km and the other at 650 km. The 350 discontinuity in velocity is preluded by a low gradient in the velocity increase from 250 - 350 km. At 350 km there is a sudden increase in the mantle compressional velocity from 8.7 km/sec to 9.6 km/sec, the velocity of compressional waves gradually increases with depth until 560 km, where it has the approximate velocity of 10.2 km/sec. From here the velocity rapidly increases to 10.9 km/sec at a depth of 650 km. Before the two velocity discontinuities (350 km and 650 km) we observed low velocity zones in some of our models. The accuracy of our data cannot prove or disprove the existence of these zones.

The study of later arrivals has helped limit the non-uniqueness of the solution to the compressional velocity structure due to $dt/d\Delta$ not being monotonically increasing. The use of the regional travel time tables, instead of the Jeffreys-Bullen (1959) tables for the upper mantle, has allowed us to work with our velocity model for a specific region, western North America. Also, by taking advantage of the Monte Carlo inversion technique for $dt/d\Delta$ data, we were able to obtain limits on the possible ranges in the velocity-depth profile.

In this study we have supported the accumulating

evidence for an azimuthal dependence of apparent velocity at LASA. Application of our empirical correction for azimuth to our $dt/d\Delta$ values reduced the scatter in our measurements over all azimuths and distances. This fact suggests that the major portion of our $dt/d\Delta$ variation with azimuth may be a result of LASA substructure.

For LASA we may have reached the useful limit of this array until we are able to make better corrections for LASA crustal and upper mantle structure as well as source region heterogeneity. These corrections might be brought about by calibration of the array over different distances and azimuths with the assistance of nuclear events. Also, such an experiment may provide us with the empirical correction needed to make an amplitude-distance study with the array.

REFERENCES

Barazangi, M., and J. Dorman (1969). World seismicity maps compiled from ESSA, Coast and Geodetic Survey, Epicenter Data, 1961-1967, Bull. Seism. Soc. Am., 59, 369-380.

Birch, F., R.F. Roy, and E.R. Decker (1968). Studies of Appalachian Geology: Northern and Maritime, Chap. 33, Heat Flow and Thermal History in New England and New York.

Borcherdt, C.A., and J.C. Rollor (1967). Preliminary Interpretations of Seismic-Refraction Profile Across the Large Aperture Seismic Array, Montana, Tech. Letter 2, National Center for Earthquake Research.

Briscoe, H., and P. Fleck (1965). Data recording and processing for the experimental large aperture seismic array, Proc. I.E.E.E., 53, 1852-1859.

Brown, T.G., and J.M. Poort (1965). Sub-surface studies and shallow-hole preparation LASA area, eastern Montana, TR 65-21, The Geotechnical Corporation, Garland, Texas.

Bullen, K. (1960). A new method of deriving seismic velocity distributions from travel-time data, Geophys. J., 3, 258-264.

Bullen, K. (1963). An Introduction to the Theory of Seismology, Cambridge University Press.

Capon, J., R. Greenfield, R. Kolker and R. Lacoss (1968). Short-period signal processing results for the large aperture seismic array, Geophys., 33, 452-472.

Carder, D., N. Gordon, and J. Jordan (1966). Analysis of surface foci travel times, Bull. Seism. Soc. Am., 52, 1037-1046.

Chinnery, M., and N. Toksöz (1967). P-wave velocities in the mantle below 700 km, Bull. Seism. Soc. Am., 57, 199-226.

Christensen, J.I., and R.S. Crosson (1968). Seismic anisotropy in the upper mantle, Tectonphysics, 6, 93-107.

Crosson, R.S., and N.I. Christensen (1969). Transverse isotropy of the upper mantle in the vicinity of Pacific fracture zones, Bull. Seism. Soc. Am., 59, 59-72.

Dowling, J., and O. Nuttli (1964). Travel time curves for a low-velocity channel in the upper mantle, Bull. Seism. Soc. Am., 54, 1981-1996.

Efroyson, M.A. (1960). Multiple regression analysis, Chap. 17 in Mathematical Methods for Digital Computers, New York.

Fairborn, J. (1968). Mantle P and S wave velocity distribution from $dt/d\Delta$ measurements, Ph.D. Thesis, Massachusetts Institute of Technology, Cambridge.

Green, P., R. Frosch, and C. Romney (1965). Principles of an experimental large aperture seismic array (LASA), Proc. I.E.E.E., 53, 1821-1833.

Green, R., and A. Hales (1968). The travel times of P waves to 30° in the central United States and upper mantle structure, Bull. Seism. Soc. Am., 58, 267-289.

Greenfield, R., and R. Sheppard (1969). The Moho depth variations under LASA and their effect on $dt/d\Delta$ measurements, Bull. Seism. Soc. Am., 59, 409-420.

Guttenberg, B. (1953). Wave velocities at depths between 50 and 500 kilometers, Bull. Seism. Soc. Am., 43, 223-232.

Herrin, E., E.P. Arnold, B.A. Bolt, G.E. Clawson, E.R. Engdahl, H.W. Freedman, D.W. Gordon, A.L. Hales, J.R. Lobdell, O. Nuttli, C. Romney, J. Taggart, and W. Tucher (1968). Special number - 1968 Seismological Tables for P phases, Bull. Seism. Soc. Am., 58, 1193-1351.

Herrin, E., and J. Taggart (1962). Regional variations in P_n velocity and their effect on the location of epicenters, Bull. Seism. Soc. Am., 52, 1037-1046.

Jeffreys, H., and K. Bullen (1958). Seismological Tables, British Assoc. for the Advancement of Science, Gray Milne Trust, London.

Johnson, L. (1967). Array measurements of P velocities in the upper mantle, J. Geophys. Res., 72, 6309-6326.

Jordan, J., R. Black, and C.C. Bates (1965). Patterns of maximum amplitudes of P_n and P waves over regional continental areas, Bull. Seism. Soc. Am., 55, 693-720.

Julian, B., and D. Anderson (1968). Travel times, apparent velocities and amplitudes of body waves, Bull. Seism. Soc. Am., 58, 334-366.

Kanamori, H. (1967). Upper mantle structure from apparent velocities of P waves recorded at Wakayama Micro-Earthquake Observatory, Bull. Earthquake Res. Inst., 45, 657-678.

Lehmann, I. (1962). The travel times of the longitudinal waves of the Logan and Blanca explosions and their velocities in the upper mantle, Bull. Seism. Soc. Am., 52, 519-526.

Lehmann, I. (1964). On the velocity of P in the upper mantle, Bull. Seism. Soc. Am., 54, 1097-1103.

Lewis, B., and R. Meyer (1968). A seismic investigation to the west of Lake Superior, Bull. Seism. Soc. Am., 58, 565-596.

Lincoln Laboratory Report No. LL-3 (1966). Measurement techniques, Sensor, and distance - Azimuth effects on LASA Amplitude Anomalies.

Lincoln Laboratory Report No. LL-6 (1967). Travel-time Anomalies at LASA.

Mack, H. (1969). Nature of short-period P-wave signal

variations at LASA, J. Geophys. Res., 74, 3171-3181.

Niazi, M., and D. Anderson (1965). Upper mantle structure of western North America from apparent velocities of P waves, J. Geophys. Res., 70, 4633-4640.

Pakiser, L.C., and J.S. Steinhart (1964). Explosion seismology in the western hemisphere, Research in Geophysics, Chap. 5, p. 123.

Romney, C.F., B.G. Brooks, R.H. Mansfield, D.C. Carder, J.N. Jordan, and D.W. Gordon (1962). Travel times and amplitudes of principal body phases recorded from Gnome, Bull. Seism. Soc. Am., 52, 1057-1074.

Roy, R.F., D.D. Blackwell, and F. Birch (1968). Heat generation of plutonic rocks and continental heat flow provinces, Earth and Planetary Science letter 5(198), p. 1-12.

Schmucker, U. (1964). Anomalies of geomagnetic variations in the south-western United States, J. Geomag. and Geoelec., 15, 193-221.

Seismic Data Laboratory, Teledyne Inc., LASA Travel-Time Data at the SDL, Report No. 172, 1966.

Sheppard, R.M. (1967). Values of LASA time station residuals, velocity and azimuth errors, Lincoln Laboratory technical note, 1967-44.

Steinhart, J.S., and R.P. Meyer (1961). Explosion Studies of Continental Structure, Carnegie Inst., Washington, Publ. 622.

Toksöz, M.N., M. Chinnery, and D. Anderson (1967). Inhomogeneities in the earth's mantle, Geophys., J. R. Astro. Soc., 13, 31-59.

Wiggins, R. (1969). Monte Carlo inversion of body-wave observations, J. Geophys. Res., 74, 3171-3181.

Woolard, G. (1959). Crustal structure from gravity and seismic measurements, J. Geophys. Res., 64, 1521-1544.

Wright, J., E. Carpenter, and R. Savill (1962). Some studies of the P waves from the underground nuclear explosions, J. Geophys. Res., 67, 1155-1160.

Zeitz, I., C. Hearn, and D. Plouff (1968). Preliminary interpretation of aeromagnetic and gravity data near the Large Aperture Seismic Array, Montana, Open File Report, U.S. Geological Survey.

Zeitz, I., E. King, W. Geddes, and E. Lidiak (1966). Crustal study of a continental strip from the Atlantic Ocean to the Rocky mountains, Geol. Soc. Am., 77, 1427-1447.